Article

Origin and function of bitumen coated torpedo jars from the Sasanian to early Islamic period fort of Fulayj in Oman

Jacques Connan *, Priestman Seth P., Engel Michael H., Zumberge Alex M., Gazmend Elezi H., Al-Jahwari Nasser S

Posted Date: 29 October 2024

doi: 10.20944/preprints202410.2158.v1

Keywords: bitumen; torpedo jar; Sasanian; Fulayj; Oman; steranes; terpanes; isotopes (C,H); biodegradation; natural asphalts; Iran; red wine

Article

Origin and Function of Bitumen Coated Torpedo Jars from the Sasanian to Early Islamic Period Fort of Fulayj in Oman

Jacques Connan [1,*], Seth Priestman [2], Michael H. Engel [3], Alex Zumberge [4], Gazmend Elezi [5,6] and Nasser S. Al-Jahwari [7]

[1] Université de Strasbourg, 23 rue Antoine de Saint-Exupéry, 64000, France
[2] Department of Archaeology, Durham University, South Road, Durham DH1 3LE, UK
[3] School of Geocsciences, The University of Oklahoma, 100 Esat Boyd Street, Norman, OK 73019, USA
[4] GeoMark Research Inc., 9748 Whithorn Drive, Houston, TX 77095, USA
[5] Pasarow Mass Spectrometry Laboratory, UCLA, 760 Westwood Plaza, Los Angeles, CA 90024, USA
[6] Cotsen Institute of Archaeology, UCLA, 308 Charles E Young Dr N, Los Angeles, CA 90024, USA
[7] Department of Archaeology, Sultan Qaboos University, Al Seeb, Al Khoudh, Muscat OM 123, Oman
* Correspondance : connan.jacques@orange.fr

Abstract: Geochemical and isotopic analysis of the bitumen lining of torpedo jar sherds from the Sasanian to early Islamic period fort of Fulayj in Oman confirms the presence of two distinct compositional categories that can be matched to contemporary sources in different areas of southwest Iran. It appears that the bitumen used to line jars was extracted from different geographic areas, hinting at the existence of multiple production locations for this vessel class. On the function of the jars, organic residue analysis provides a positive identification of biomarkers associated with the storage and transport of red wine. These results provide the first published confirmation of the long suspected association between torpedo jars and wine transportation from the core urbanised zone of the Sasanian and early Islamic imperial heartlands towards the Persian Gulf and Indian Ocean maritime sphere. The results have added significance as the samples are derived from relatively accurately dated archaeological contexts spanning the period before and after the Islamic conquest.

Keywords: bitumen; torpedo jar; Sasanian; Fulayj; Oman; steranes; terpanes; isotopes (C,H); biodegradation; natural asphalts; Iran; red wine

1. Introduction

A sample of 15 sherds of bitumen coated torpedo jars have been selected for analysis from the late Sasanian to early Islamic period fort of Fulayj in Oman. Torpedo jars form a distinctive class of handless transport container vessels with a narrow mouth and a pointed base coated with a waterproof lining. They are found very widely distributed across the Mesopotamian plain, southern Iran and along the Persian Gulf and western Indian Ocean littoral. Isolated examples are also attested from shipwreck assemblages in Southeast Asia. Inconviently, their chronology is broad spanning the period from at least the 3rd to 9th centuries CE with little obvious stylistic, morphological or technical change. Recent research on the composition of both the ceramic fabric and bitumen lining provides evidence for the production of this class within the general area of southern Iraq and/or southwest Iran [1–4]. The potential to further refine our knowledge of the production location(s) of this class remains open to investigation. The current contribution adds to this body of research by analysing samples from securely dated contexts from the fort of Fulayj in Oman.

2. Archaeological Context

Fulayj is the site of a small c. 30 × 30m, heavily defended, square fortification with projecting 'U' shaped corner and entrance flanking towers and a single entranceway facing to the east. It was built

 doi:10.20944/preprints202410.2158.v1

with a thick, neatly constructed stone base most likely supporting a much more substantial mudbrick superstructure. Radiocarbon dating indicates that the fort was built in the late pre-Islamic period sometime between the early 5th and mid-6th century CE [5]. The latest results of excavation and dating indicate that there was a brief horizon of related activity in the same location preceding the fort construction. The location of the site is c. 30km southwest of the major Indian Ocean emporium of Sohar, which may already have attained some prominence before the Islamic conquest. The dating of the fort, its clear architectural links with similar small Late Antique fortlets across the Middle East, and its expert construction all strongly suggest that it was built by an external military force, which we can associate historically with the projection of Sasanian imperial power and the settlement of a Persian population on the Batinah during the late Sasanian period [6]. It is not clear if this was a long-lived military occupation. Finds within the fort are generally scarce. Significantly, the building underwent certain modifications and continued to be occupied during the first century following the Islamic conquest [7]. At this time mudbrick rooms were inserted into one corner of the fort and the defensive aspect of the gateway was modified. It is possible that the site took on a less overtly military function. Torpedo jar samples derive from contexts spanning both the earlier and later occupation.

3. Materials and Methods

3.1. Samples

Fifteen samples of bitumen coating the interior face of potsherds were isolated by scraping the surface with a scalpel (Table 1). Four examples of the samples are presented in Figure 1. They illustrate different sitiations with variable crusts of bitumen. No bitumen occurs on the exterior face of the potsherds.

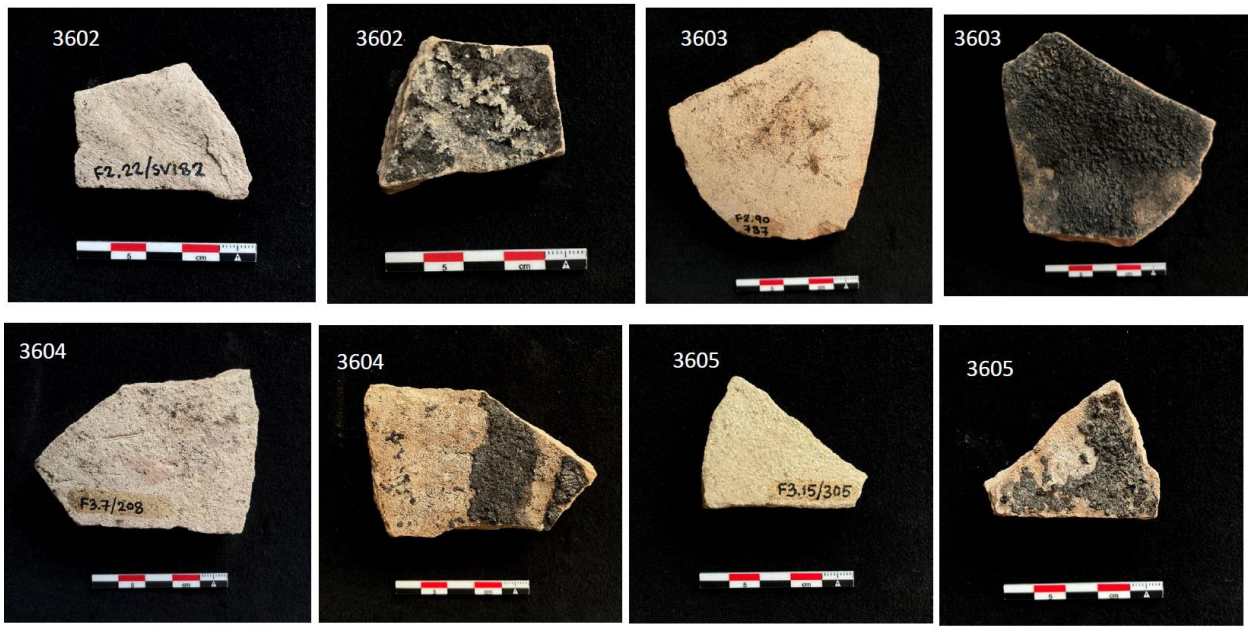

Figure 1. Picture of four samples of Fulayj showing various aspects of the bitumen coating the interior face of potsherds.

Table 1. Basic information on the samples.

Site	Country	Archaeological Reference	Phase	Date Range	Wine Biomarkers	Bitumen Source	Lab Number	Reference Number
Fulayj	Oman	F2.041/FN405	2a	Mid-3rd - mid-6thC		Kermanshah	3458	1
		F2.051/FN626	2a	Mid-3rd - mid-6thC	Yes	Kermanshah	3460	3
		F2.059/FN596	2a	Mid-3rd - mid-6thC		Kermanshah	3461	4
		F2.059/FN610	2a	Mid-3rd - mid-6thC		Khuzistan	3462	5

 doi:10.20944/preprints202410.2158.v1

F3.022/FN475	2a	Mid-3rd - mid-6thC		Kermanshah	3606	13
F3.023/FN512	2a	Mid-3rd - mid-6thC		Khuzistan	3607	14
P.012/FN423	2c	Early 5th - mid-6thC	Yes	Khuzistan	3465	8
F2.090/FN787	2c	Early 5th - mid-6thC		Khuzistan	3603	10
F2.042/FN513	3	Mid-6th - late 7thC	Yes	Kermanshah	3459	2
F3.015/FN305	3	Mid-6th - late 7thC		Khuzistan	3605	12
P.011/FN316	4a	Residual post 7thC	Yes	Khuzistan	3463	6
P.011/FN338	4a	Residual post 7thC	Yes	Kermanshah	3464	7
F2.022/SV182	4a	Residual post 7thC		Kermanshah	3602	9
F3.007/FN208	4a	Residual post 7thC		Khuzistan	3604	11
R.003/FN123	4b	Residual post 7thC		Khuzistan	3608	15

3.Analytical Procedures

3.2.1. Bitumen Analysis

All archaeological and geological bituminous samples were subjected to the same analytical procedure at GeoMark Research Ltd. Detailed procedures have been described in previous papers [3,8].

3.2.2. Wine Detection

The LC-MS/MS analysis follows a new analytical technique that targets ancient wine biomarkers developed at the UCLA Pasarow Mass Spectrometry Laboratory) (Elezi et al. in preparation), [9].

The archaeological samples were pulverized in a pestle and mortar, and 2 g of pottery powder was treated with 5 mL of Methanol/DI Water/Formic Acid mixture 50:50:0.1 (v/v/v) in a glass test tube. The samples were vortexed and centrifuged at 2000 xg for 15 min, and the supernatants were transferred into new tubes. The extraction procedure was repeated by adding 3 mL of the mixture, and the supernatants were pulled into the new tubes. 100 pmoles of Daidzin solution in Ethanol were added as an internal standard for potential quantification analysis, and then the samples were dried in a vacuum concentrator for 4 hours. The dried samples were resuspended in 100 µl of Methanol/Water/Formic Acid (95:5:01) (v/v/v), vortexed thoroughly, and centrifuged at 2000 xg for 5 min. The supernatant was transferred to HPLC polypropylene vials, and 25 µl was injected for analysis.

A targeted Liquid Chromatography-Tandem Mass Spectrometry (LC-MS/MS) assay was developed on a Linear Ion Trap LTQ-XL (Thermo Scientific) mass spectrometer coupled to a Dionex Ultimate 300 HPLC system (Thermo Scientific) through a reversed-phase GL Science analytical column (Inert Sustain 2 µm, Phenyl 150 x 2.1 mm). The instrument was optimized in positive ion mode monitoring transitions for Malvidine 3-glucoside (Mv3g) 493-331 m/z, Vitisin A (VA) 561-399 m/z, Vitisin B (VB) 517-355 m/z, and Daidzin (DA) 417-255 m/z). The mobile phase consisted of A (99.9:0.1 *v/v* Water/Formic Acid) and B (99.9:0.1 *v/v* Acetonitrile/Formic Acid). The HPLC method utilized the linear gradient mixture of eluents A and B to elute the targeted compounds (min/%B: 0/5, 5/5, 12/40, 26/75, 28/5, 40/The m/z of a fragment ion from each compound was monitored at a specific LC retention time to ensure their specificity and accurate identification.

4. Results

4.1. Gross Composition

Gross composition data are listed in Table 2 Extractable Organic matter in dichloromethane (EO % by weight/sample), which represents the amount of bitumen, ranges between 9.8 and 51% by weight with an average value of 37.9%. All samples are rather rich in bitumen.

 doi:10.20944/preprints202410.2158.v1

Table 2. Gross composition of the dichloromethane extract (EO in % by weight /sample) and isotopic data: 13C (‰ / VPDB) and D (‰ / VSMOW). Significance of abbreviations: sat = saturated hydrocarbons, aro = aromatic hydrocarbons, NSO= resins, asp = asphaltenes, pol = polars = resins + asphaltenes.

sample number	Geomark reference	location	country	EO %/sample	%sat	%aro	%HC	%NSO	%asp	%pol	total	$d^{13}C$ sat	$d^{13}C$ aro	$d^{13}C$ NSO	$d^{13}C$ asp	dDNSO average	dDasp average	
3458	UNK0934	Fulaj	Oman	50.5	1.8	2	3.8	9	87.2	96.2	100	-27.9	-26.8	-26.9	-26.5	-83	-76	oleanana pas d'oleanane
3459	UNK0935			39.4	1.7	2	3.7	11.3	85	96.3	100	-27.7	-26.8	-27	-26.7	-84	-76	
3460	UNK0936			43.7	1.9	2.2	4.1	8.2	87.7	95.9	100	-27.3	-26.6	-26.8	-26.5	-83	-89	
3461	UNK0937			40.8	2	2.9	4.9	18.6	76.5	95.1	100	-27.5	-27.8	-27.1	-26.5	-85	-75	
3462	UNK0938			15.1	3.3	6	9.3	37.1	53.6	90.7	100	-27.3	-27.1	-28.1	-28.1	-97	-91	
3463	UNK0939			38.0	1	1.6	2.6	9	88.4	97.4	100	-29	-28	-28	-27.9	-75	-68	
3464	UNK0940			58.9	2.2	1.6	3.8	7	89.2	96.2	100	-27.6	-26.8	-26.8	-26.3	-80	-79	
3465	UNK0941			35.4	1.4	2.6	4	11.7	84.3	96	100	-28.4	-27.8	-27.9	-27.9	-83	-67	
3602	UNK1119			47.8	2.1	2.1	4.2	13.4	82.4	95.8	100	-27.5	-26.3	-27.1	-26.7	**-106**	**-84**	
3603	UNK1120			39.6	1.8	1.3	3.1	8.6	88.3	96.9	100	-28.8	-27.5	-27.6	-27.8	**-88**	**-73**	
3604	UNK1121			45.6	4.9	3.3	8.2	11.8	80.1	91.8	100	-29.1	-27.3	-27.2	-27.8	**-115**	**-77**	
3605	UNK1122			37.3	1.1	1.4	2.5	8.9	88.6	97.5	100	-28.8	-27.6	-27.9	-27.8	**-99**	**-79**	
3606	UNK1123			9.8	3.6	3.6	7.2	20.9	71.9	92.8	100	-27.6	-26.1	-27.1	-26.7	**-107**	**-83**	
3607	UNK1124			43.7	1.9	1.8	3.7	11.9	84.3	96.3	100	-28.7	-27.1	-28	-28	**-100**	**-75**	
3608	UNK1125			23.1	1.2	1.7	2.9	9.5	87.6	97.1	100	-28.1	-27.6	-28.3	-28	**-96**	**-74**	
				13.019 21 37.9														

A plot of % sat (saturated hydrocarbons) vs. % aro (aromatic hydrocarbosn) vs. % polars (= resins + asphaltenes) in Figure 2, shows that most samples are extremely rich in polars. One sample (No. 3462) is slightly different for enriched in hydrocarbons (9.3 %).

 doi:10.20944/preprints202410.2158.v1

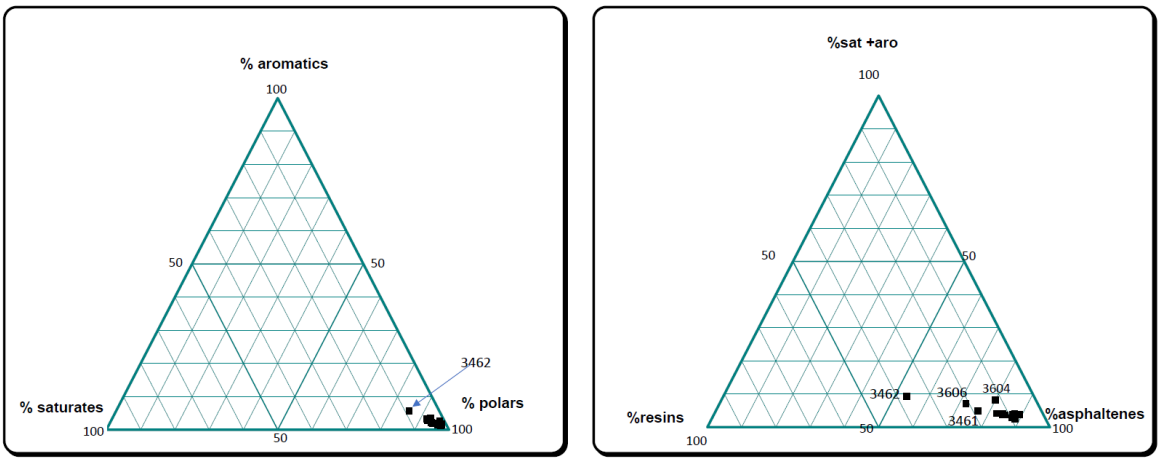

Figure 2. Gross composition of the dichloromethane extract in two ternary diagrams: % saturates vs. % aromatics vs. % polars and % sat + aro vs. % resins vs. % asphaltenes.

A plot of % sat + aro vs. % resins (NSO's) vs. % asphaltenes shows a diversified situation with samples extremely rich in asphaltenes (more than 80%) and some others (No. 3462, 3606 and 3451) in which resins are higher, between 18.6 and 37.1 %. The compositions of archaeological samples characterized by an enrichment in asphaltenes has been reported in many publications [10–24].

4.2. Isotope Data

Carbon and hydrogen isotopes are presented in Table 3 The plot of 13Csat vs. 13Caro and 13CNSO vs. 13Casp in Figure 3, clearly shows that there is at least two main groups of bitumen, group one with 13Casp between -27.1 and -26.8 ‰/VPDB and group two with 13Casp between -28.3 and -27.2 ‰/VPDB. Comparison of these values with data acquired on oil seeps from Iran (Figure 4) confirms the occurrence of two main group of samples originating from different geographical locations. Group one corresponds to samples originating mainly from Khuzestan and Bushehr, group two to samples from Kermanshah, Ilam, and Lorestan.

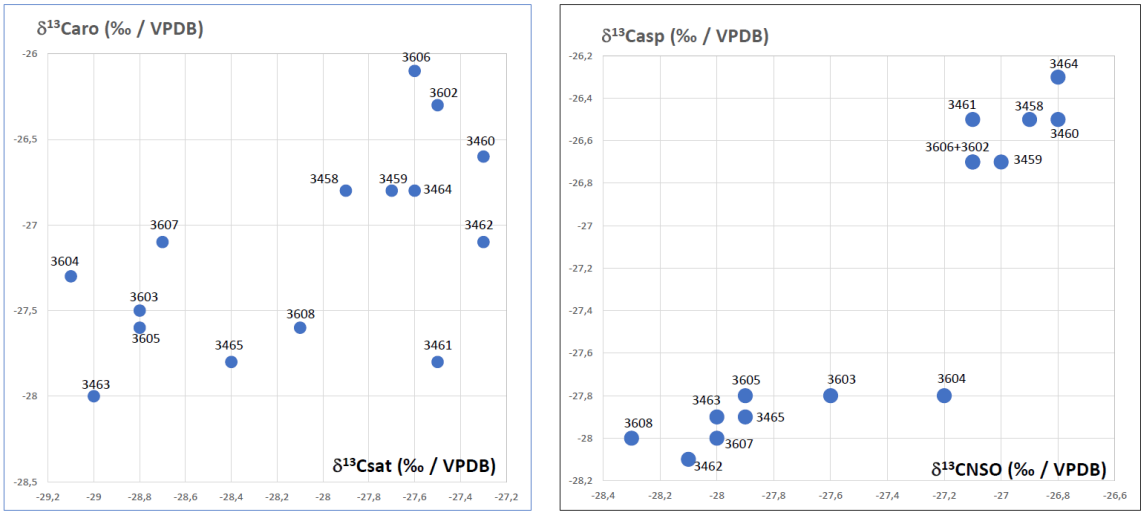

Figure 3. Plot of 13C (‰ / VPDB) of aromatics vs. 13C (‰ / VPDB) of saturates and 13C (‰ / VPDB) of asphaltenes vs. 13C (‰ / VPDB) of NSO for the Fulayj samples.

Preprints.org (www.preprints.org) | NOT PEER-REVIEWED | Posted: 29 October 2024 doi:10.20944/preprints202410.2158.v1

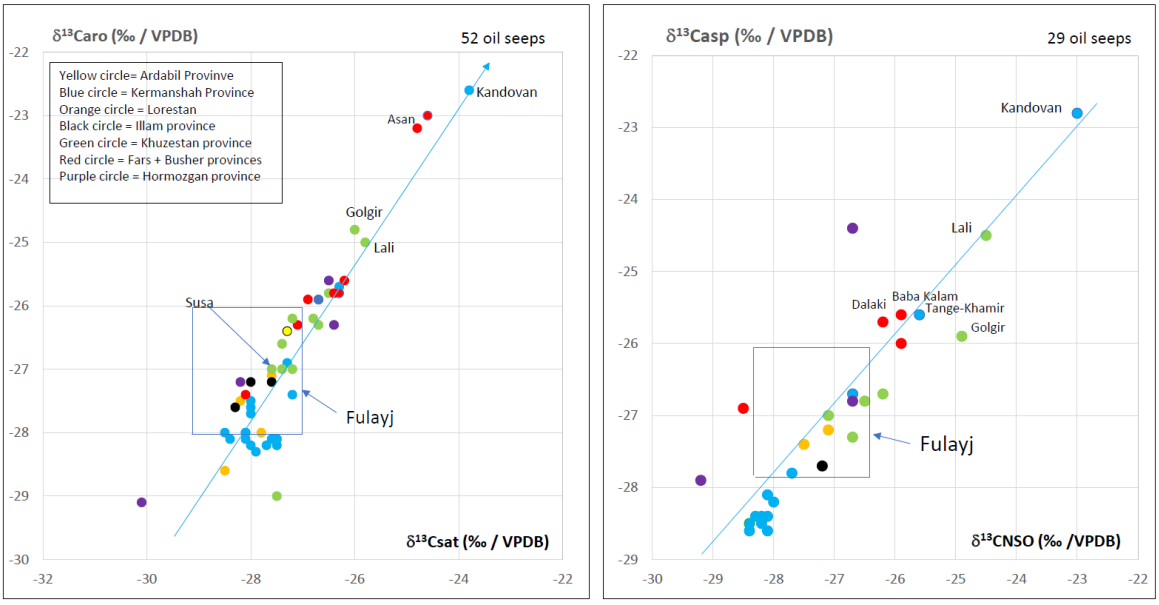

Figure 4. Plot of 13C (‰ / VPDB) of aromatics vs. 13C (‰ / VPDB) of saturates and 13C (‰ / VPDB) of asphaltenes vs. 13C of NSO for the oil seeps of Iran: Comparison with the Fulayj 's data.

The plot of Dasp vs DNSO in Figure 5a does not show any relationship between D values and their group, defined by their carbon isotope ratios. This feature is not surprising for these parameters are not source dependant but reflects oxidation intensities among bitumens [25]. Comparison of Fulayj data (Figure 5a) with those of 15 oil seeps from Iran (Figure 5b) shows that the Fulayj asphaltenes are generally more oxidized than those of oil seeps. Surprisingly and not explained, resins (NSO) of Fulayj are comparable to those of oil seeps of Iran.

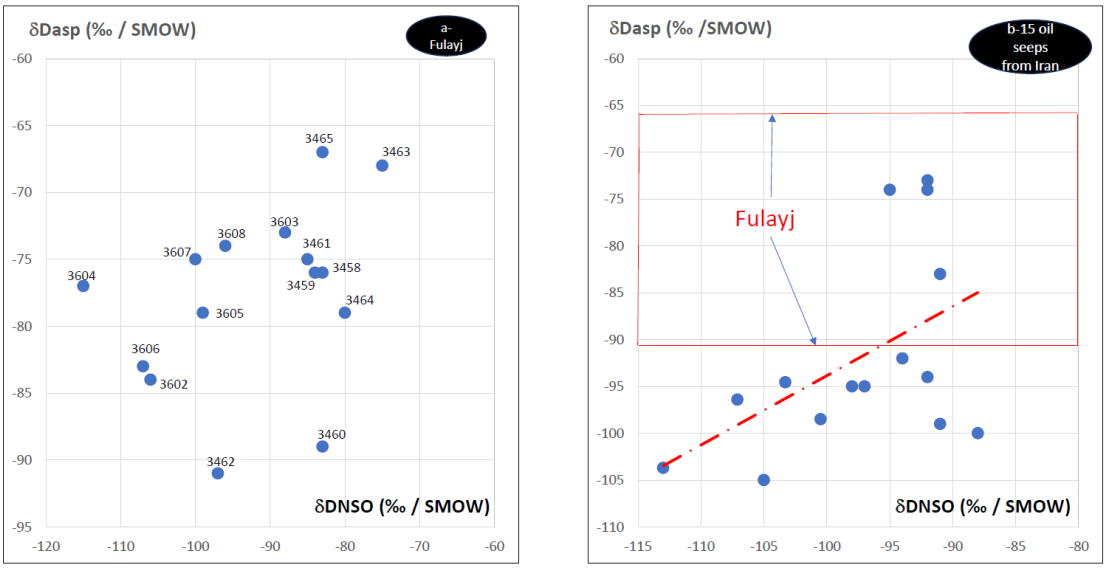

Figure 5. Plot of the D (‰ / VSMOW) of asphaltenes vs. D (‰ / VSMOW) of NSO. a) data on Fulayj. b) data on 15 oil seeps from Iran.

Table 3. Molecular data on steranes and terpanes. Significance of abbreviations: C30αβHopane=17α,21β-hopane, OL/H = 18α(H)-oleanane / hopane, GA/C31αβHR = Gammacerane/ 17α,21β,22R-30-homohopane, ster/terp = steranes / terpanes, Dia /reg = diasteranes / regular steranes, %C27αββR+S = 5α,14β,17β-20R+20S-cholestane, %C28αββR+S= 5α,14β,17β-20R+20S-24methylcholestane, %C29αββR+S=5α,14β,17β-20R+20S-24ethylcholestane, C29ααα20S/20R=

 doi:10.20944/preprints202410.2158.v1

5α,14α,17α-20S-24ethylcholestane / 5α,14α,17α-20R-24ethylcholestane, C29H/C30H = norhopane/ hopane, C27Ts/Tm = 18α-22,29,30-trisnorneohopane / 17α-22,29,30-trisnorhopane, C35S/C34S = C34-17α,21β-22S-extended hopane /C35- 17α,21β-22S-extended hopane.

lab number	Geo Mark number	site	C30 Hpm	Tet/C23	C29/H	OL/H	C31R/H	GA/H	GC35S/C34S	ster/Terp	Dia/Reg	% C27	% C28	% C29	C29 20S/R	C29ab/aaR	Ts/Tm	tricyclics	terpanes	steranes	C27diasteranes	c29aaaRsterane
3458	UNK09 34	Fula yj	2001	2.01	0.96	0.13	0.38	0.3	0.11	1.3	0.27	0.72	11.1	30.2	58.7	1.39	1.68	0.52	almost absent	well preserved	biodegraded	present	altered
3459	UNK09 35	Fula yj	642	1.08	0.93	0.16	0.37	0.44	0.16	1.94	0.37	0.84	10.4	26.4	63.2	1.94	1.6	0.44	almost absent	slightly biodegraded?	biodegraded	present	altered
3460	UNK09 36	Fula yj	575	1.35	1.02	0.33	0.37	0.41	0.15	2.14	0.65	1.41	11.6	28.1	60.2	2.88	3.95	0.61	almost absent	biodegraded	biodegraded	present	altered
3461	UNK09 37	Fula yj	157	0.94	1.13	0.27	0.36	0.44	0.16	3.47	0,,18	0.87	15.5	26.7	57.8	2.78	1.07	0.46	almost absent	biodegraded	biodegraded	traces	altered
3462	UNK09 38	Fula yj	1632	1.09	1	0	0.38	0.67	0.25	1.11	0.04	0.33	18.7	23.1	58.2	0.28	0.46	0.14	almost absent	well preserved	preserved	traces	preserved
3463	UNK09 39	Fula yj	13716	6.63	0.93	0	0.33	0.63	0.21	0.99	0.06	0.05	19.8	20.6	59.6	0.64	0.94	0.11	almost absent	well preserved	preserved	absent	preserved
3464	UNK09 40	Fula yj	1321	1.06	0.96	0.15	0.38	0.25	0.09	1.51	0.57	1.26	17	31	52	1.44	2.03	0.6	almost absent	well preserved	slighly biodegraded?	abundant	altered
3465	UNK09 41	Fula yj	5556	3.57	1.24	0	0.31	0.68	0.21	1.18	0.1	0.15	13.8	23.3	62.9	0.85	1.15	0.19	almost absent	well preserved	preserved?	traces	preserved
3602	UNK11 19	Fula yj	2536	1.55	0.75	0.14	0.4	0.25	0.1	1.19	0.2	0.88	11.2	29.1	59.8	1.3	1.96	0.5	absent	well preserved	biodegraded	low present	biodegraded
3603	UNK11 20	Fula yj	11306	3.21	1.1	0	0.38	0.61	0.23	1.11	0.09	0.08	26.2	24.8	49	0.53	1.04	0.19	almost absent	well preserved??	almost absent	preserved

Preprints.org (www.preprints.org) | NOT PEER-REVIEWED | Posted: 29 October 2024 doi:10.20944/preprints202410.2158.v1

3604	UNK11 21	Fulayj	2424	1.94	1.18	0	0.32	0.63	0.2	0.9	0.2	1.73	21.4	31.7	46.9	0.73	1.12	0.27	absent	well preserved	preserved	abundant	preserved
3605	UNK11 22	Fulayj	9480	5.72	1.14	0	0.34	0.66	0.22	1.88	0.07	0.1	14.6	24.2	61.2	0.57	0.86	0.18	absent	well preserved	biodegraded	traces	preserved
3606	UNK11 23	Fulayj	1617	1.12	0.9	0.12	0.42	0.39	0.16	1.81	0.14	1.21	11.8	23.2	65	1.74	1.71	0.43	absent	well preserved?	biodegraded	present	biodegraded
3607	UNK11 24	Fulayj	16149	3.66	1.04	0	0.34	0.56	0.19	0.99	0.07	0.09	24.6	21.7	53.7	0.59	0.94	0.15	almost absent	well preserved	biodegraded?	traces	preserved
3608	UNK11 25	Fulayj	1723	1.35	1.19	0	0.31	0.9	0.28	2.78	0.13	0.26	6.4	20.1	73.5	1.72	1.58	0.18	almost absent	well preserved?	biodegraded	traces	bioegraded

4.3. Steranes and Terpanes

Steranes and terpanes were used as biomarkers to characterize the source of bitumen. Mass fragmentograms of terpanes (m/z 191) and steranes (m/z 217) of two archaeological samples (No. 3463 and No. 3460) are reproduced in Figure Terpanes of the No. 3463 sample show a complete pattern of the hopane family (C28 H to C35 H) with a high Tm/Ts ratio, a rather high gammacerane, almost no tricycloplyprenanes. Their steranes is dominated by regular steranes which are slightly biodegraded. Terpanes from No. 3460 show also the complete hopane family with occurrence of tricyclopolyprenanes (28/3 and 29/3), a low gammacerane and the occurrence of 18 (H)-oleanane which reflects the contribution of the Pabdeh Tertiary formation in the source rocks which have produced this type of bitumen. One should notice that the occurrence of 18 (H)-oleanane is matching with samples having 13C of asphaltenes between -26 and -27 ‰/VPDB (Figures 6 and 7).

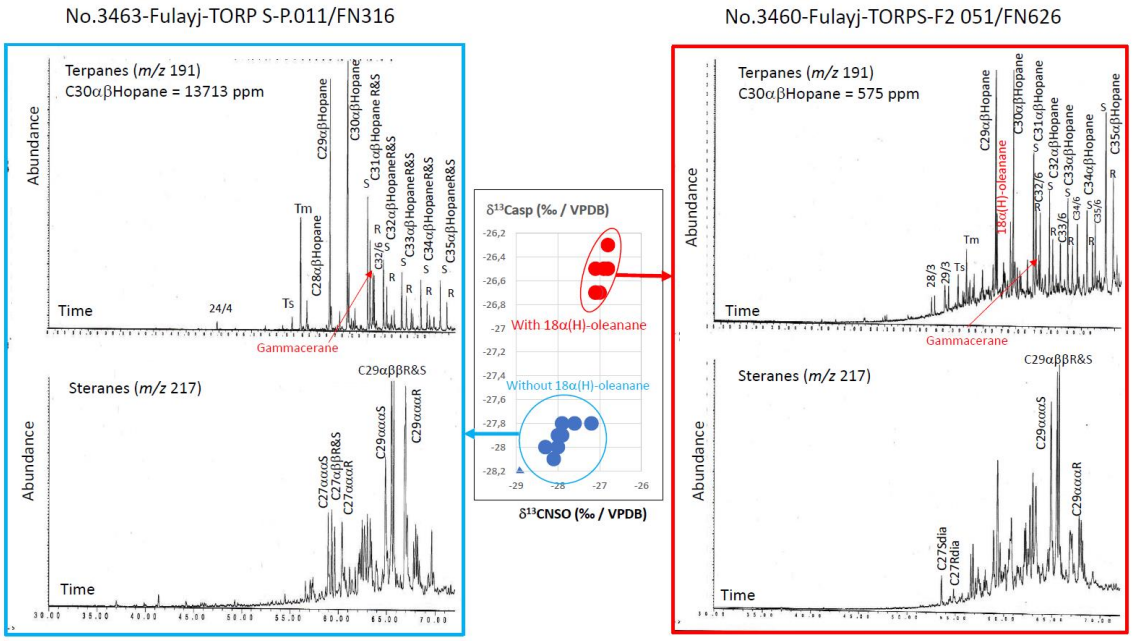

Figure 6. Mass fragmentograms of steranes (*m*/z 217) and terpanes (*m*/z 191) with the plot of δ^{13}Casp vs. δ^{13}CNSO : comparison of the sample No.3643 without 18α(H)-oleanane to the sample No.3460 with 18α(H)-oleanane.

Preprints.org (www.preprints.org) | NOT PEER-REVIEWED | Posted: 29 October 2024 doi:10.20944/preprints202410.2158.v1

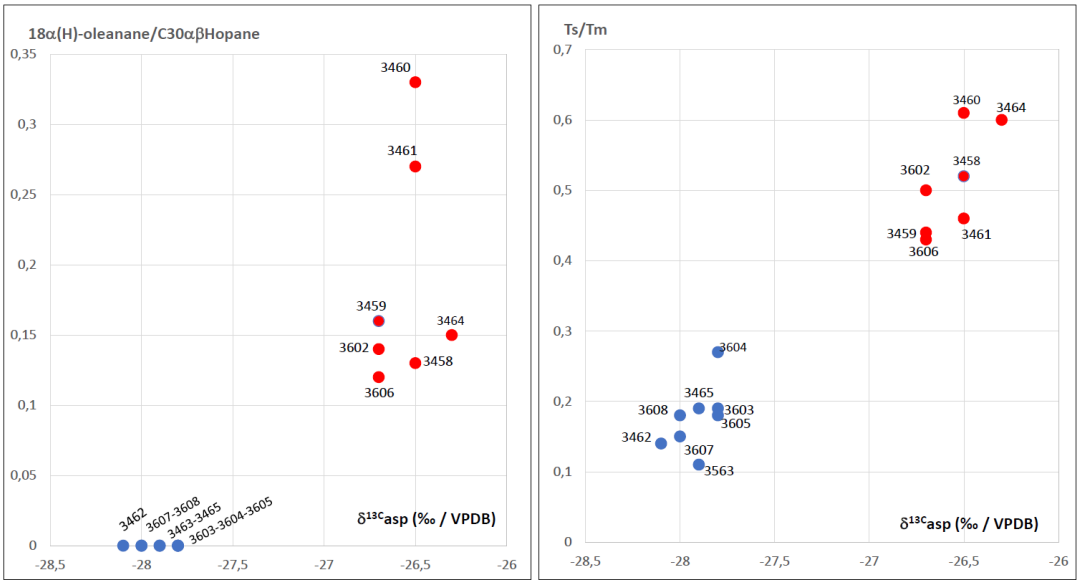

Figure 7. Plot of 18α(H)-oleanane / C30αβHopane *vs.* δ^{13}Casp (‰ / VPDB) and Ts/Tm *vs.* δ^{13}Casp (‰ / VPDB) with the Fulayj samples.

The plot of some characteristic ratios namely Ts/Tm vs. 13C of asphaltenes (Figure 7), Ts/Tm vs. Diasteranes/Regular steranes and Ts/Tm vs. Gammacerane/C31 RHopane confirms the occurrence of at least two bitumen families. The first one (No. 3458, 3459, 3460, 3461, 3464, 3602 and 3606) corresponds to bitumen containing 18 (H)-oleanane, high diasteranes/regular steranes, high Ts/Tm ratio, low gammacerane/C31 RHopane and occurrence of tricyclic terpanes. This family was generated from a source rock (likely the Eocene-Oligocene Pabdeh formation) in which the organic matter has a vegetal contribution, and is deposited in a marine environment under anaerobic conditions [26]. The second family (No. 3462, 3463, 3465, 3603, 3604, 3605, 3607, 3608) has a low Ts/Tm ratio, mainly regular steranes , a high gammacerane/C31 Rhopane and originates likely from the Albian-Aptian Khazdumi formation deposited in a very anoxic hypersaline marine environment [27,28].

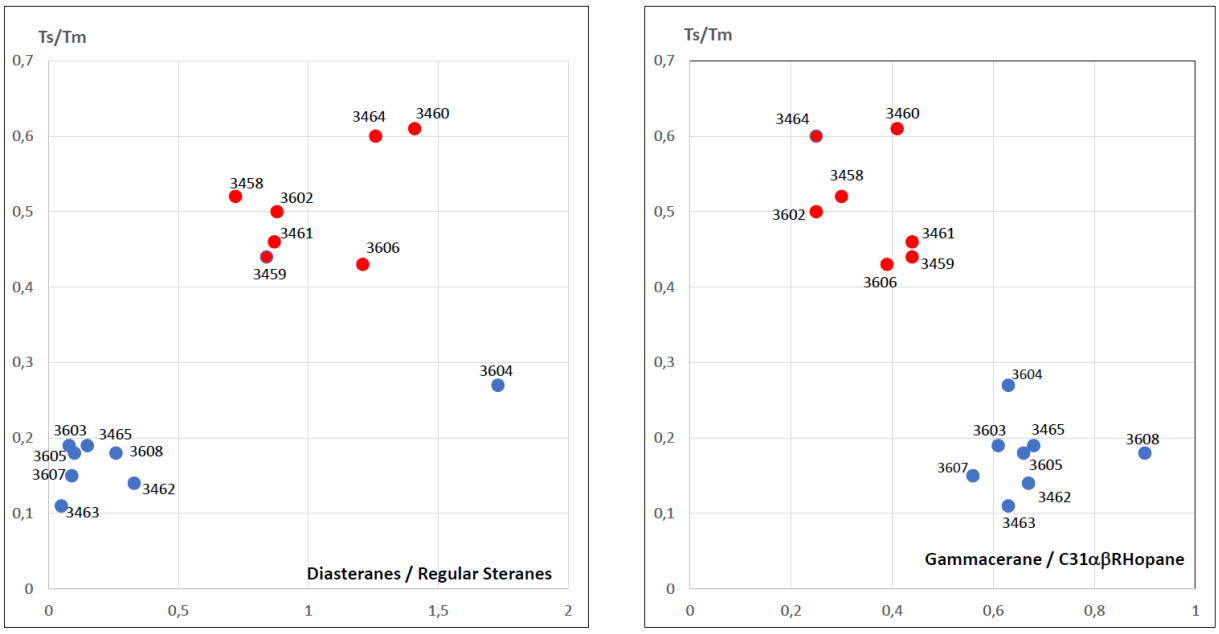

Figure 8. Plot of Ts/Tm *vs.* Diasteranes/Regular steranes and Ts/Tm vs. Gammacerane/ C31αβRHopane with the samples of Fulayj.

 doi:10.20944/preprints202410.2158.v1

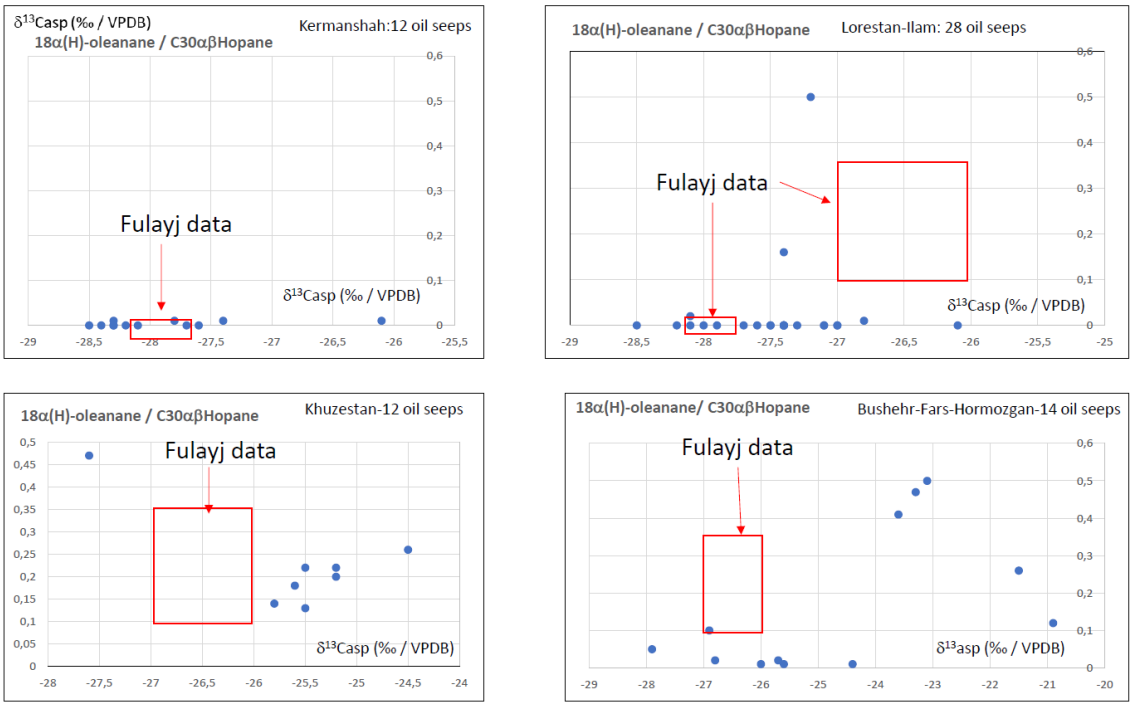

Figure 9. Plot of 18α(H)-oleanane / C30αβHopane *vs.* δ^{13}Casp (‰ / VPDB) in oil seeps from different provinces of Iran.

Comparison of Fulayj data to those of oil seeps and solid bitumen analyzed in the different provinces of Iran shows that the first group matches data from natural asphalts from Karmanshah and Lorestan-Illam provinces whereas the second group is not matching the present day acquired data on oil seeps from Lorestan-Illam-Khuzestan-Busher-Fars and Hormozgan provinces. Utilization of data on archaeological sites as proxis in Figure 10, reveals that data from Fulayj are matching data from Susa in Khuzestan and Chogah Ahowan in Ilam.

Preprints.org (www.preprints.org) | NOT PEER-REVIEWED | Posted: 29 October 2024 doi:10.20944/preprints202410.2158.v1

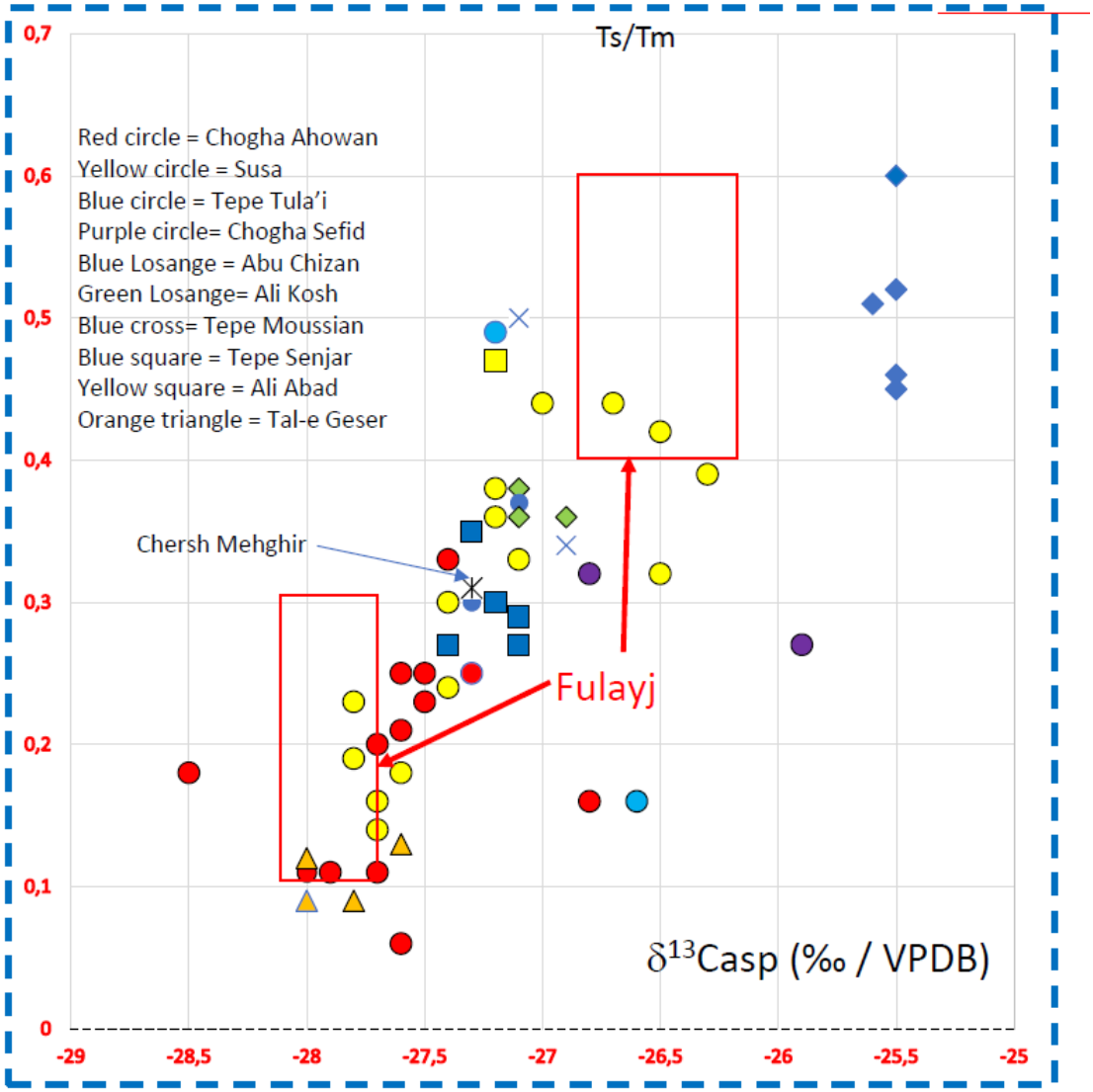

Figure 10. Plot of 18 (H)-oleanane / C30 Hopane vs. 13Casp (‰ / VPDB) in bitumen from archaeological sites of Iran.

Plot of data on steranes in Figure 11 discriminates again the two groups of samples. Samples with 18 (H)-oleanane are more biodegraded than samples without 18 (H)-oleanane as indicated by the reduced C27 steranes . Samples without 18 (H)-oleanane have less C28 steranes as is often the case in samples with high gammacerane which display a V-pattern (C28<C27 and C29). Interesting, samples with 18 (H)-oleanane shows the selective removal of the C29 R sterane, a characteristic biodegradation effects seen elsewhere in archaeological samples: at Kuriki Höyük in Turkey, Qala't al Bahrain and Saar in Bahrain, Hummal in Syria, Anuradhapura in Sri Lanka [1,29–31]. This selective biodegradation of the biological configuration of steranes has been observed in crude oils at depth [32] and has been reproduced in 15 days under laboratory conditions using grams-positive strains belonging to Nocardia and Arthrobacter genera [33,34].

Preprints.org (www.preprints.org) | NOT PEER-REVIEWED | Posted: 29 October 2024 doi:10.20944/preprints202410.2158.v1

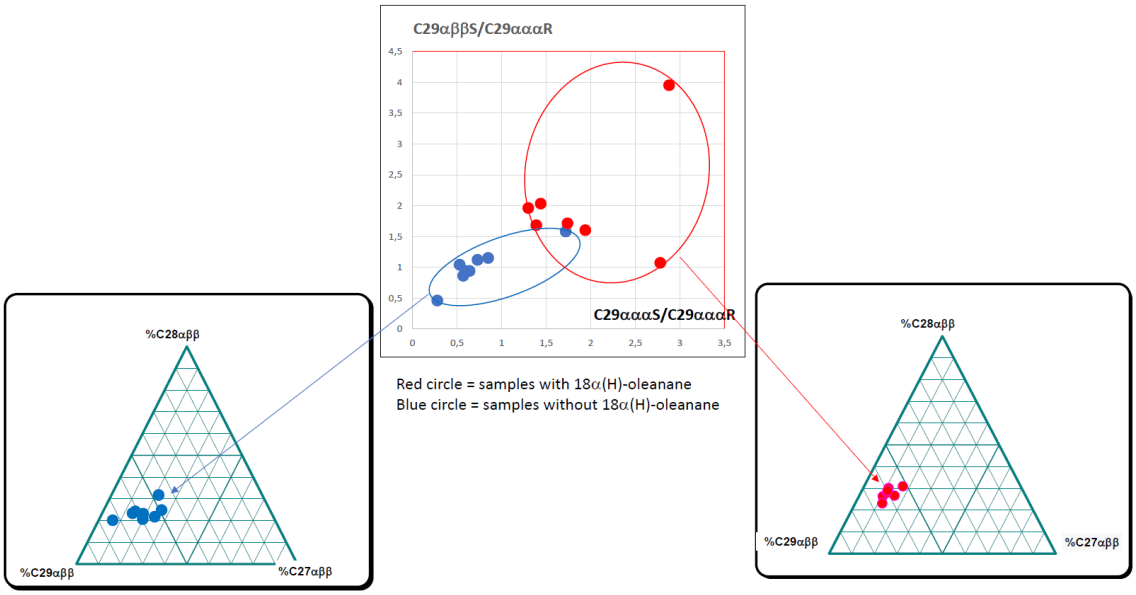

Figure 11. Plot of αββsteranes in a ternary diagram : %C27 vs. %C28 vs. %C29 and plot of C29αββS/C29αααR vs. C29αααS/C29αααR: comparison of samples with (red circle) and without 18α(H)-oleanane (blue circle).

4.5. Identification of Wine

In an ongoing research program conducted by Gazmend Elezi at the UCLA Pasarow Mass Spectrometry Laboratory, a targeted LC-MS/MS assay was developed to detect wine residues [9]. The method targeted wine biomarkers such as Malvidine 3-glucoside (Mv3g), Vitisin A (VA), and Vitisin B (VB) monitoring transitions from precursors (Mv3g 493 m/z, VA 561 m/z, VB 517 m/z) to product ions (OE, 331 m/z, VA 339 m/z VB 355 m/z) (Figure 12). These molecules are characteristics of red wine [35,36].

 doi:10.20944/preprints202410.2158.v1

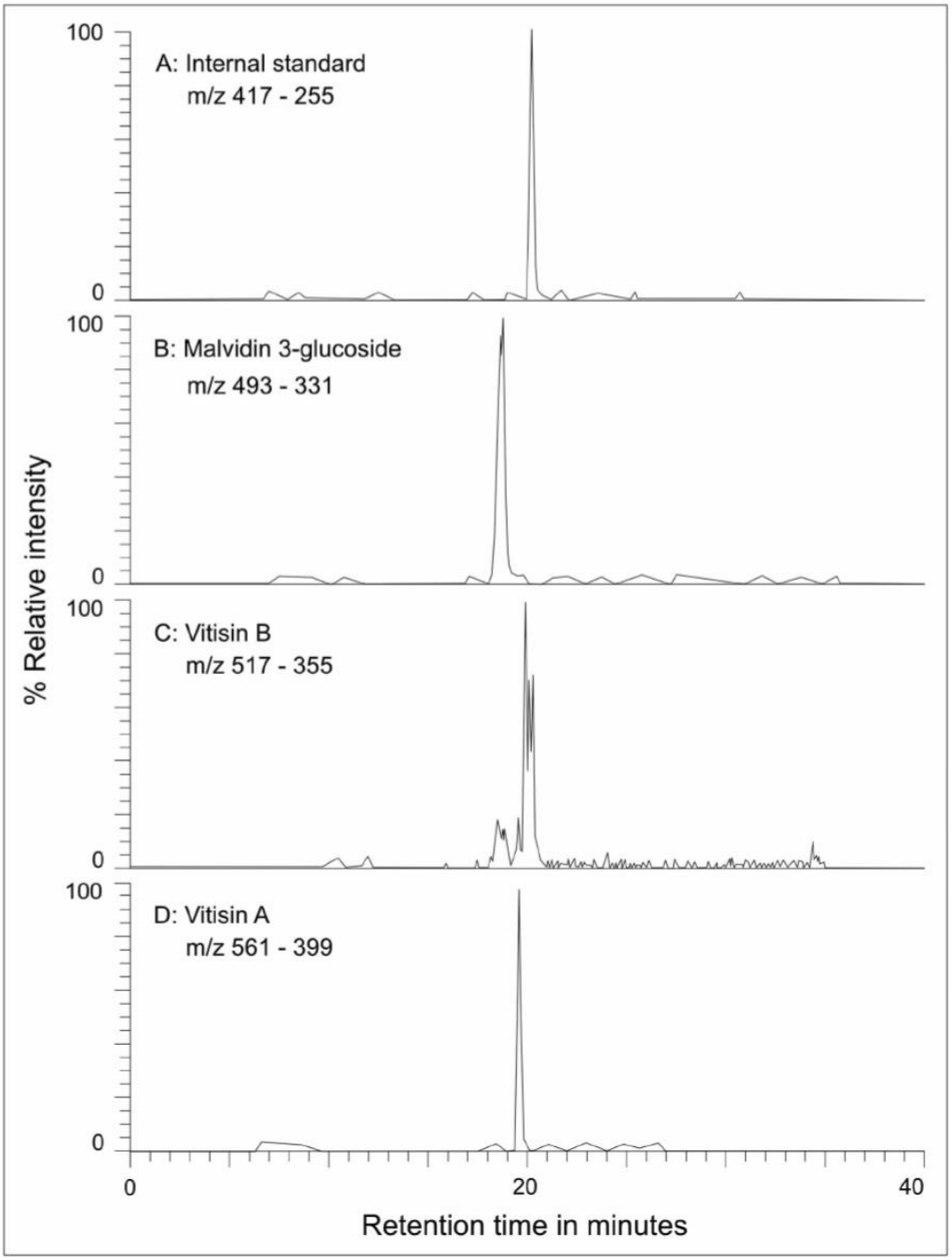

Figure 12 LC-MS/MS reference chromatogram of the commercial analytes depicting the signals of the monitored precursor-product ion transitions for the targeted compounds and the internal standard.

Positive answers were recorded for 5 samples: 3 (Nos 3459, 3460 and 3464) with bitumen containing 18 (H)-oleanane and 2 (Nos 3453 and 3465) with bitumen without 18 (H)-oleanane (Table 4, Figure 13). Sample No. 3459 comes from within a room securely dated to the 7th century AD, seemingly directly following the conversion to Islam.

 doi:10.20944/preprints202410.2158.v1

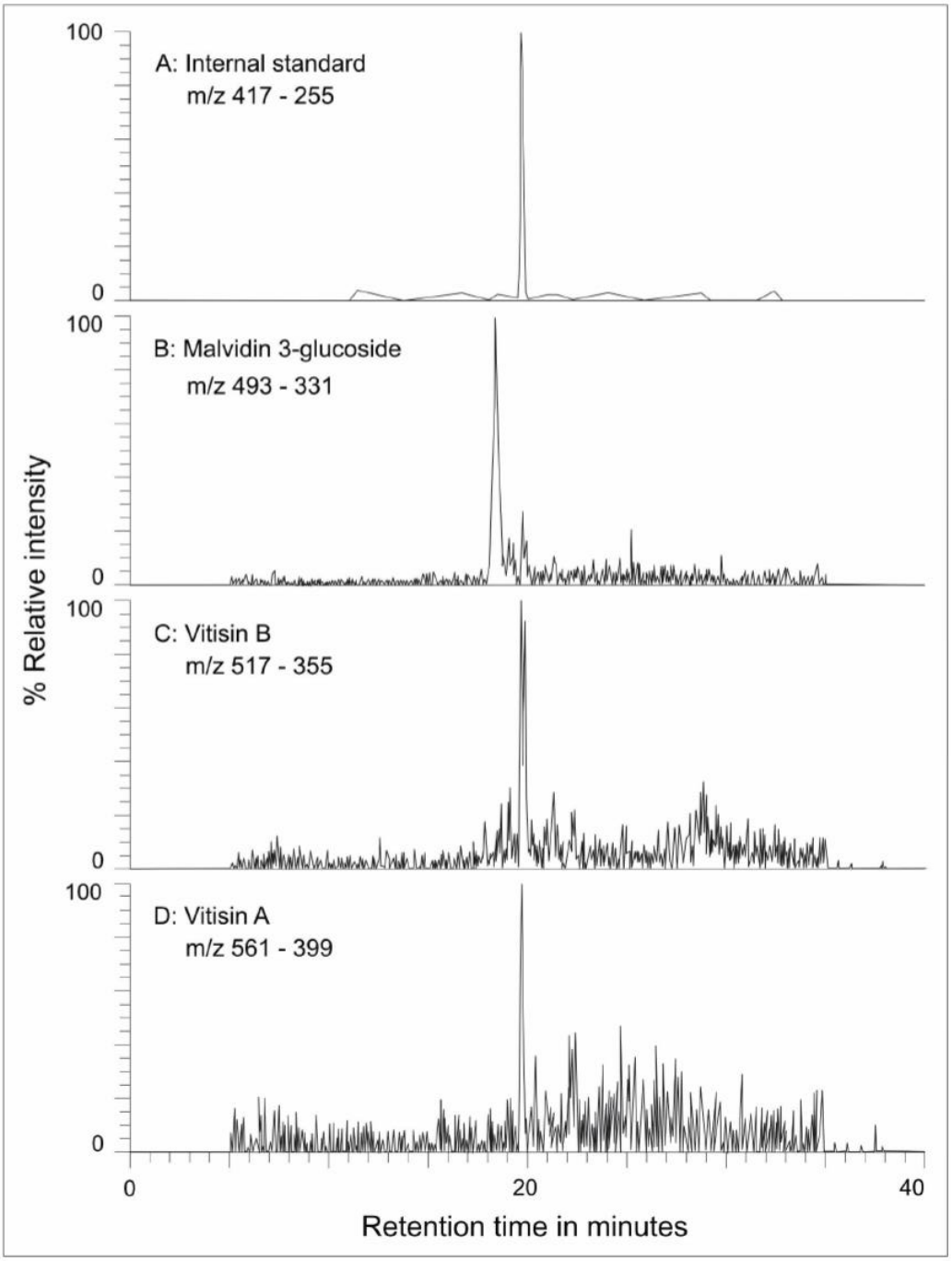

Figure 14. LC-MS/MS chromatogram of the archaeological sample 3464 depicting the signals of the monitored precursor-product ion transitions for the targeted compounds and the internal standard.

Table 4. Wine biomarkers detected on archaeological samples. Samples were spiked with a known concentration of Daitzin, which was used as internal standard.

lab number	site	Malvidin 3-Glucoside	Vitisin A	Vitisin B	Daidzin (Internal standard)
3458	Fulayj	absent	absent	absent	present
3459	Fulayj	absent	absent	present	present
3460	Fulayj	absent	absent	present	present
3461	Fulayj	absent	absent	absent	present

 doi:10.20944/preprints202410.2158.v1

3462	Fulayj	absent	absent	absent	present
3463	Fulayj	present	absent	present	present
3464	Fulayj	present	absent	present	present
3465	Fulayj	present	absent	present	present

5. Conclusions

Fifteen samples of bitumen coated torpedo jars have revealed two main compositional groups originating in southwest Iran, one from the Karmanshah- Lorestan provinces and the other from the Khuzestan-Illam provinces. Five of these potsherds were identified as wine containers on the basis of specific biomarkers associated with red wine. The interpretation of this relatively small sample is complicated. Both bitumen composition groups are associated with the detected traces of wine. This suggests a consistent function regardless of the location of production. Of course, an important caveat here is that the origin of the bitumen and location of pottery production may not necessarily have been the same. Chronologically, the samples are associated with different parts of the occupation sequence (Table 1), the dating of which is constrained by radiocarbon dating evidence. Not all of this is fully published, but the outline can be summarised. One of the sherds that provided a positive identification for the presence of wine comes from Phase 2a (No. 3460). This is a thin but particularly rich occupation horizon that predates the construction of the fort indicating some kind of earlier activity. The absolute dating evidence is broad but delimited within the Sasanian period from the c. mid-3rd to mid-6th century CE. It would be surprising if the dating is in fact very much earlier than the construction of the fort. A second fragment (No. 3465) belongs to Phase 2c, which comprises the ephemeral occupation directly connected with the use of the fort sometime between the early 5th to mid-6th century CE. A third sample (No. 3459) belongs to the re-occupation of the fort and the modification of its interior with the insertion of a domestic mudbrick buiding in Phase 3, which can be dated between the late 6th to late 7th century certainly covering the first decades of the Islamic transition. The remaining samples are associated with the gradual collapse of the fortification and we assume that these fragments are residual from any part of the earlier occupation. In terms of differing sources of bitumen composition, there does not appear to be any strong chronological correlation. One should be cautious in drawing any firm conclusions from this limited dataset. What the results do seem to point to is both a consitency in the pattern of usage of this vessel class through time, and to the enduring acquisition of bitumen from multiple sources. This might plausibly be connected with alternative manufacturing centers and the distribution of different regional varieties of wine as outlined in the contemporary historigraphy. These features require further systematic investigation at scale.

Acknowledgments: The Fulayj Fort Project was co-directed by Seth Priestman, Nasser al-Jahwari, Eve MacDonald and Derek Kennet. Permission to conduct analysis of the samples was kindly facilitated by the Ministry of Heritage and Tourism of the Sultanate of Oman and Sultan Qaboos University. We thank the many specialists who contributed to the archaeological interpretation of the site that underpins the results that are reported here.

References

1. Stern, B., Connan, J., Blakelock, E., Jackman, R., Coningham, R.A.E., Heron, C. From Susa to Anuradhapura: reconstructing aspects of trade and exchange in bitumen-coated ceramic vessels between Iran and Sri Lanka in the Third to the Ninth centuries AD. Archaeometry 50, 3, **2008**, 409-428.
2. Connan, J., Priestman, S., Vosmer, T., Komoot, A., Tofighian, H., Ghorbani, B., Engel, M.H., Zumberge, A., Van de Velde, T. Geochemical analysis of bitumen from West Asian torpedo jars from the c. 8th century Phanom-Surin shipwreck in Thailand. Journal of Archaeological Science, **2020**, 117, 105111. https://doi.org/10.1016/j.jas.2020.105111
3. Connan, J., Engel, M.H., Jackson, R., Priestman, S., Vosmer, T., Zumberge, A. Geochemical Analysis of Two Samples of Bitumen from Jars Discovered on Muhut and Masirah Islands (Oman). Separations **2021**, 8,10,182. https://doi.org/103390/separations8100182

4. Tomber, R., Spataro, M., Priestman, S. Early Islamic Torpedo Jars from Siraf: Scientific Analyses of the Clay Fabric and Source of Indian Ocean Transport Containers. Iran, **2022**, 60, 2, 240-63. https://doi.org/10.1080/05786967.2020.1792797
5. Priestman, S., al-Jahwari, N., MacDonald, E., Kennet, D., Alzeidi, K., Andrews, M., Dabrowski, V., Kenkadze, V., MacDonald, R., Mamalashvili, T., Al-Maqbali, I., Naskidashvili, D., Rossi, D. Fulayj: A Sasanian to Early Islamic Fort in the Sohar Hinterland. Proceedings of the Seminar for Arabian Studies, **2023**, 52, 291-304.
6. 6. al-Jahwari, N., Kennet, D. Priestman, S., Sauer, E. Fulayj: A Late Sasanian Fort on the Arabian Coast. Antiquity, **2018**, 92, 363, 724-41. https://doi.org/10.15184/aqy.2018.64
7. Priestman, S.M.N. The archaeology of Early Islam in Oman: Recent Discoveries from Fulayj on the Batinah. The Anglo-Omani Society Review, **2019**, 40-43.
8. Connan, J. ; Adelsberger, K.A. ; Engel, M. ; Zumberge, A. Bitumens from Tell Yarmuth (Israel) from 2800 BCE to 1100 BCE : A unique case history for the study of degradation effects on the Dead Sea bitumen. Organic Geochemistry 168, **2022**, 104392. https://doi.org/10.1016/orggeochem.2022.104392
9. Elezi, G., H. Barnard, H., Whitelegge, J. Novel method for the detection of ancient wine biomarkers in archaeological pottery, In preparation.
10. Forbes, R. J. Studies in Ancient Technology. Volume 1: Bitumen and Petroleum in Antiquity. **1955**, Leiden: E. J. Brill.
11. Marschner, R.F., Wright, H.T. Asphalt from Middle Eastern Archaeological Sites. Archaeological Chemistry 1, Advances in Chemistry Series, **1978**, Chicago, 97-112.
12. Connan J. Le bitume dans l'Antiquité. **2012**, Arles: Errance, Actes Sud.
13. Connan, J., Nissenbaum, A., Dessort, D. Molecular archaeology: Export of Dead Sea asphalt to Canaan and Egypt in the Chalcolithic-Early Bronze Age (4th-3rd millennium BC). Geochimica et Cosmochimica Acta, **1992**, 56, 2743-2759
14. Connan, J., Nishiaki, Y. The bituminous mixtures of Tell Kosak Shamali on the Upper Euphrates (Syria) from the Early Ubaid to the Post Ubaid: Composition of mixtures and origin of bitumen. In: Nishiaki, Y., Matsutani, T. (Eds.), Tell Kosak Shamali-The Archaeological Investigations on the Upper Euphrates, Syria, Chalcolithic Technology and Subsistence. The University Museum and The University of Tokyo, Tokyo, Japan, **2003**, Vol.II, Chapter 18, pp. 283-306.
15. Connan, J., Nissenbaum, A., Imbus, K., Zumberge, J., Macko, S. Asphalt in iron age excavations from the Philistine Tel Miqne-Ekron city (Israel) : Origin and trade routes. Organic Geochemistry 37, **2006**, 1768-1786. https://doi.org/10.1016/j.orggeochem.2006.08.015
16. Connan, J., Carter, R. A geochemical study of bituminous mixtures from Failaka and Umm an-Namel (Kuwait), from the Early Dilmun to the Early Islamic period. Arabian Archaeology and Epigraphy, **2007**, 18, 1–43.
17. Connan, J., Kavak, O., Sağlamtimur, H., Engel, M., Zumberge, A., Zumberge, J. A geochemical study of bitumen residues on ceramics excavated from Early Bronze graves (3000-2900 BCE) at Başur Höyük in SE Turkey. Organic Geochemistry, **2018**, 115, 1-11. https://doi.org/10.1016/j.orggeochem.2017.09.007
18. Connan, J., Adelsberger, K.A., Engels, M.H., Zumberge, A. Bitumens from Tell Yarmuth (Israel) form 2800 BCE to 1100 BCE: A unique case history for the study of degradation effects on the Dead Sea bitumen. Organic Geochemistry 168, **2022**, 104392. https://doi.org/10.1016/j.orggeochem.2022.104392
19. Nissenbaum, A., Connan, J. Application of organic geochemistry to the study of Dead Sea asphalt in archaeological sites from Israel and Egypt. In: Pike, S., Gitin, S. (Eds.), The Practical Impact of Science on Near Eastern and Aegean Archaeology., Wiener laboratory Publication, 3, **1999,** Archetype Publications Ltd, London, 91-98.
20. Schwartz, M., Hollander, D. The Uruk expansion as dynamic process: A reconstruction of Middle to Late Uruk exchange patterns from bulk isotope analyses of bitumen artifacts. Journal of Archaeological Science: Reports 7**, 2016**, 884-899.
21. Schwartz, M., Hollander, D., Stein, G.J. Reconstructing Mesopotamian exchange networks in the 4th millenium BC: geochemical and archaeological analyses of bitumen artifacts from Hacinebi Tepe, Turkey. Paléorient 25, **2000**, 67-82.
22. Brown, K., Connan, J., Poister, K.M., Vellanoweth, R.L., Zumberge, J., Engel, M.H. Sourcing archaeological asphaltum (bitumen) from the California Channel Islands to submarine seeps. Journal of Archaeological Science 43, **2014**, 66-76.
23. Daneels, A., Romo de Vivar-Romo, A., Linares-Jurado, A., Reyes-Lezama, M., Tapia-Mendoza, E., Morales-Puente, P., Cienfuegos-Alvarado, E., Otero-Trujano, F.J. Chemical analysis of bitumen paint on classic period Central Veracruz ceramics, Mexico. Journal of Archaeological Science: Reports 17, **2018**, 657-666.
24. Wendt, C.J., Lu, S-T. Sourcing archaeological bitumen in the Olmec region. Journal of Archaeological Science 33,**2006**, 89-97. https://doi.org/10.1016/j.jas.2005.06.012
25. Charrié-Duhaut, A., Lemoine, S., Adam, P., Connan, J., Albrecht, P. Abiotic oxidation of bitumens under natural conditions. Org.Geochem. 31, **2000**, 977-1003.

26. Ashkan, S.A.M. Geochimie organique des roches mères et des huiles du basin de Zagros (Iran). Thèse, Université Henri Poincaré, Nancy I, **1998**.
27. Moldowan, J.M., Seifert, W.K., Gallegos, E.J. Relationship between petroleum composition and depositional environment of petroleum source rocks. American Association of Petroleum Geologists Bulletin,69, **1985**, 1255-1268.
28. Fu J., Sheng, G., Peng, P., Brassell, S.C., Eglinton, G., Jigang, J. Peculiarities of salt lake sediments as potential source rocks in China. Organic Geochemisty, 10, **1986**, 119-1126.
29. Connan, J., Genç, E., Kavak, O., Engel, M.H., Zumberge, A. Geochemistry and origin of bituminous samples of Kuriki Höyük (SE Turkey) from 4000 BCE to 200 CE: comparison with Kavuşan Höyük, Hakemi Use and Salat Tepe. Journal of Archaeological Science: Reports 41, **2022**, 103348.
30. Connan, J., Lombard, P., Killick, R., Højlund, F., Salles, J.F., Kalaf; A.The archaeological bitumen of Bahrain from the early Dilmun period (c. 2200 BC) to the sixteenth century AD: a problem of source and trade. Arab. Archeol.Epigr 9, **1998**, 141-181.
31. Boëda , E., Connan, J., Muhesen, S. Bitumen as hafting material on Middle Paleolithic artefacts from the El Kown Basin, Syria . In: Akazawa, T., Aoki, K., Bar Yosef, O. (Eds.), Neanderthals and Modern Humans in Western Asia, Plenum , New York, **1998**, pp.181-204.
32. 32 Seifert, W., Moldowan, M., Demaison, G., Source correlation of biodegraded oils. Org.Geochem. 6, **1984**, 633-643.
33. Chosson, P., Connan, J., Dessort, D., Lanau, C. In vitro biodegradation of steranes and terpanes: a clue to understanding geological situations. In Albrecht P., Moldowan, M., Philp, P. (Eds.). Biological markers in sediments and petroleum, Prentice-Hall, Englewood Cliffs, **1991a**, pp.320-349.
34. Chosson, P., Lanau, C., Connan, J., Dessort, D. Biodegradation of refractory hydrocarbons from petroleum under laboratory conditions. Nature 351, **1991b**, 640-642.
35. Morata, A., Calderón, F., González, M. C., Gómez-Cordovés, M.C., Suárez., J.A. "Formation of the Highly Stable Pyranoanthocyanins (Vitisins A and B) in Red Wines by the Addition of Pyruvic Acid and Acetaldehyde." Food Chemistry 100 (3): **2007**, 1144–52. www.https://doi.org/10.1016/j.foodchem.2005.11.024
36. De Freitas, V., Mateus., N. Formation of pyranoanthocyanins in red wines: a new and diverse class of anthocyanin derivatives. Anal. Bioanal. Chem. 401, **2011**, 1463-1473. www.https://doi.org/10.1007/s00216-010-4479-9